

Probing Electrostatic Potentials in Solution with Carbon Nanotube Transistors

Lisa Larrimore,[†] Suddhasattwa Nad,[‡] Xinjian Zhou,[†] Héctor Abruña,^{*,‡} and Paul L. McEuen^{*,†}

Laboratory of Atomic and Solid State Physics and Department of Chemistry and Chemical Biology, Cornell University, Ithaca, New York 14853

Received January 23, 2006; Revised Manuscript Received April 21, 2006

ABSTRACT

We have used single-walled carbon nanotube transistors to measure changes in the chemical potential of a solution due to redox-active transition-metal complexes. The interaction of the molecules with a gold electrolyte-gate wire changes the electrostatic potential sensed by the nanotube, which in turn shifts the gate-voltage dependence of the nanotube conductance. As predicted by the Nernst equation, this shift depends logarithmically on the ratio of oxidized to reduced molecules.

Electrochemists have developed a variety of tools for investigating and characterizing redox-active molecules in solutions. These techniques generally depend on the measurement or control of potential and current. Potentiometric techniques probe the electrochemical potential $\bar{\mu}_i$, which is composed of the electrostatic (φ) and chemical (μ_i) potentials:

$$\bar{\mu}_i = q\varphi + \mu_i \quad (1)$$

Amperometric techniques (i.e., measurements of current) provide information related to reaction rates. The combination of current and potential measurements results in powerful techniques, such as cyclic voltammetry, for determining reaction rates (current) as a function of driving force (applied potential).¹ In recent times, there has been a drive toward ultraminiaturization of electrochemical systems for sensor applications and for studying small collections of molecules where the detection of discrete events might be possible.

Carbon nanotubes (NTs) are promising candidates for performing nanoscale electrochemistry, and the use of individual NTs as working electrodes has been demonstrated.^{2,3} Semiconducting NTs can also be used as field-effect transistors (FETs) in an electrolyte environment, in which a gate wire is used to establish the electrochemical potential of the solution relative to the nanotube.^{4,5} The high sensitivity of nanotube FETs makes them excellent sensors,⁶ and electrolyte-gated NT FETs have been used to sense small

molecules,^{7,8} proteins,^{9–11} and surfactants.¹² In each of these experiments, the analyte caused a shift in the gate-voltage dependence of the nanotube conductance, which was attributed to charge transfer from adsorbed molecules to the nanotube or a local electrostatic gating effect.

Here we explore the response of electrolyte-gated single-walled carbon nanotube (SWNT) transistors to redox-active transition-metal coordination complexes. We find that the nanotube acts similarly to a reference electrode and senses changes in the electrostatic potential of the solution. These changes are directly related to the chemical potentials of the redox-active molecules, as measured in a traditional electrochemical cell. We show that although there may be some local interaction between the molecules and the SWNT FET, the primary source of the signal is the electrochemical interaction between the molecules and the electrolyte-gate wire.

Figure 1 shows an atomic force microscope (AFM) image of a SWNT and a schematic of the measurement geometry. Nanotubes were grown from iron nanoparticles patterned onto a doped Si substrate with a 200 nm oxide layer using a “fast heating” chemical vapor deposition method.¹³ Gold contacts (30 nm high) were added lithographically on top of the NTs, with the source and drain electrodes separated by 10 μm . A 50 mV bias was applied across the SWNT FET to measure the conductance.

The microfluidic system that carries redox-active molecules to the SWNT FET consists of a poly(dimethylsiloxane) (PDMS) channel 60 μm wide and 25 μm high, which was fabricated using photolithography. The PDMS was exposed to air plasma for 30 s to make the surface

* Corresponding authors. E-mail: hda1@cornell.edu (HA); mceuen@ccmr.cornell.edu (PLM).

[†] Laboratory of Atomic and Solid State Physics, Cornell University.

[‡] Department of Chemistry and Chemical Biology, Cornell University.

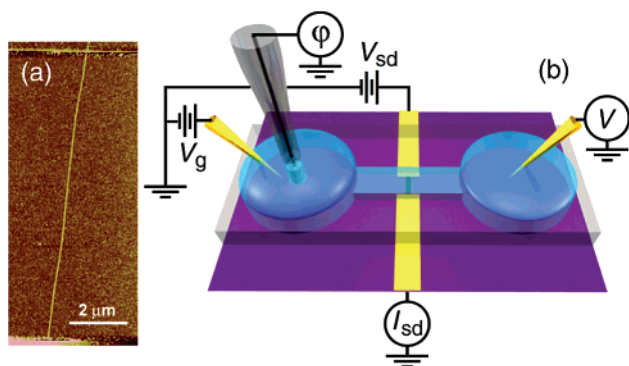


Figure 1. (a) AFM image of a SWNT between two gold electrodes. The NT diameter is 2.6 nm, and its length is 10 μm . (b) Measurement schematic. An electrolyte-gate voltage, V_g , is applied to a gold wire while measuring the source-drain current with a 50 mV bias. The SWNT FET is connected to the large reservoir by a PDMS microfluidic channel. Using a high-impedance voltmeter, we can measure the electrostatic potential with a Ag/AgCl reference electrode or the electrochemical potential in the second reservoir with an additional gold wire.

hydrophilic and was then sealed on top of the SWNT FET. The channel was filled and emptied using the large reservoirs on each end. The flow direction in the channel is determined by a combination of surface tension and gravity, and could be controlled by varying the relative sizes of the droplets in each reservoir. Fluorescent tracer particles were sometimes added to observe the flow speed and direction. The PDMS was removed after each set of experiments, and each SWNT FET could be reused repeatedly.

The PDMS channel was initially filled with an aqueous NaCl solution, which was also used as the supporting electrolyte background. We applied a gate voltage, V_g , to a gold wire placed in one of the reservoirs, which establishes the electrochemical potential of the solution relative to the NT.⁵ In some experiments, we used a high-impedance voltmeter to measure the potential of a Ag/AgCl reference electrode or a second gold wire in the other large reservoir, as illustrated in Figure 1. The reference electrode probes the electrostatic potential, and the gold wire probes the electrochemical potential.

Redox-active molecules were dissolved at varying concentrations in the NaCl supporting electrolyte. Details of the synthesis and purification of the redox couples can be found in the Supporting Information. Molecules initially in an oxidized state were $[\text{Co}(\text{bpy})_3]\text{Cl}_3$ (where bpy is 2,2'-bipyridine), $\text{K}_3[\text{Fe}(\text{CN})_6]$, and $[\text{Ru}(\text{NH}_3)_6]\text{Cl}_3$; molecules initially in a reduced state were $[\text{Co}(\text{tpy})_2]\text{Cl}_2$ (where tpy is 2,2':6',2''-terpyridine), $[\text{Co}(\text{atpy})_2]\text{Cl}_2$ (where atpy is 4'-amino-2,2':6',2''-terpyridine), $[\text{Co}(\text{bpy})_3]\text{Cl}_2$, $\text{Na}_4[\text{Fe}(\text{CN})_6]$, and $[\text{Ru}(\text{NH}_3)_6]\text{Cl}_2$. These molecules were introduced into one of the reservoirs while measuring the conductance of the SWNT FET.

Figure 2 shows the response of the SWNT FETs to these redox-active molecules. The inset shows that the NT conductance changes dramatically upon the addition of each molecule solution. The main panel of Figure 2 shows that this change at $V_g = 0$ is due to a strict translation in the full G versus V_g response, which can be described as a shift in

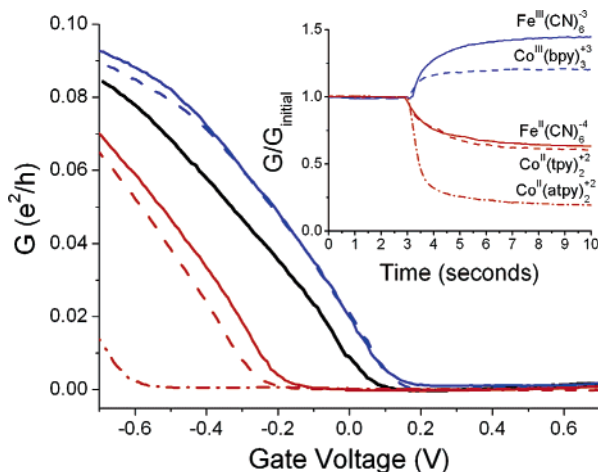


Figure 2. Adding 1 mM solutions of different redox-active molecules, all with the same 1 mM NaCl supporting electrolyte, causes a shift in the NT threshold voltage. Oxidized molecules ($\text{K}_3[\text{Fe}(\text{CN})_6]$, solid blue, and $[\text{Co}(\text{bpy})_3]\text{Cl}_3$, dashed blue) cause a positive shift from the initial curve (black), and reduced molecules ($\text{Na}_4[\text{Fe}(\text{CN})_6]$, solid red; $[\text{Co}(\text{tpy})_2]\text{Cl}_2$, dashed red; and $[\text{Co}(\text{atpy})_2]\text{Cl}_2$, dash-dot red) cause a negative shift. Some hysteresis is observed in the reverse sweep direction. The leakage current between the electrolyte-gate wire and the drain electrode, which is typically 100 times smaller than the source-drain current, has been subtracted. Inset: NT conductance as a function of time during addition of redox-active molecules, with $V_g = 0$.

the threshold voltage, V_{th} , at which the nanotube starts conducting. The direction of this translation is correlated with the redox state of the molecules and not with the overall molecular charge: oxidizing molecules cause a positive threshold voltage shift and reducing molecules cause a negative threshold voltage shift.

Figure 3 shows that we see roughly the same threshold voltage shift if the redox-active molecules are near the nanotube as we do if they are confined by the flow to the reservoir with the gate wire. The NT conductance changes as soon as the molecules are added to the reservoir with the gate wire, regardless of the flow speed or direction. In particular, the conductance still changes even if the molecules have not reached the SWNT FET by either advection or diffusion. We also see no change in conductance if the molecules are confined only to the reservoir that does not contain the gate wire.

To quantify the response, we determined the ratio of the oxidized to reduced molecules, $[\text{Ox}]/[\text{Red}]$. This was measured using a cyclic voltammogram taken with a 25 μm platinum ultramicroelectrode in a traditional electrochemical cell,¹ as shown in the upper inset of Figure 4. $[\text{Ox}]/[\text{Red}]$ was then determined directly from the ratio of the diffusion-limited currents. The $[\text{Ox}]/[\text{Red}]$ value could also be changed by performing bulk electrolysis with a large-surface-area working electrode.¹ Further experimental details are provided in the Supporting Information. Figure 4 shows the threshold voltage shift for a 100 μM $[\text{Co}(\text{tpy})_2]\text{Cl}_2$ solution at different $[\text{Ox}]/[\text{Red}]$ ratios. This shift varies with the logarithm of $[\text{Ox}]/[\text{Red}]$, with a slope of 61 ± 6 mV. This slope is also roughly 60 mV for the $[\text{Ru}(\text{NH}_3)_6]^{2+/3+}$ redox couple, but it

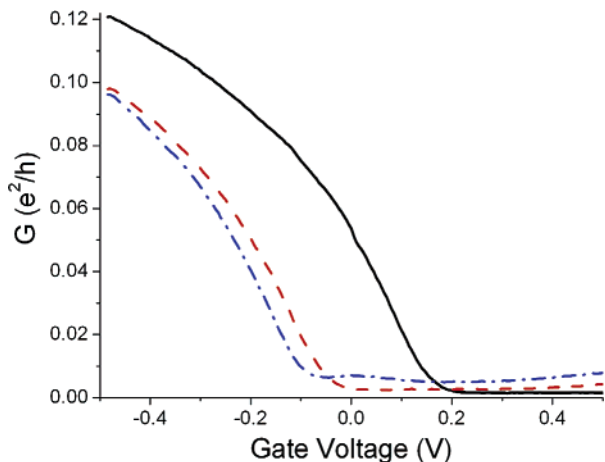


Figure 3. Threshold voltage shift does not depend on whether the molecules are near the SWNT FET. Adding 100 μM $[\text{Co}(\text{tpy})_2]\text{Cl}_2$ to a 100 mM NaCl supporting electrolyte causes roughly the same shift from the initial curve (black) when the molecules fill the entire microfluidic channel (dash-dot blue) as when they are confined by the flow to the reservoir containing the gate wire (dashed red). The small shift between the red and blue curves may be due to an interaction of the redox molecules with the nanotube or with the gold source and drain electrodes. The small current in the off state is likely caused by leakage through the electrolyte.

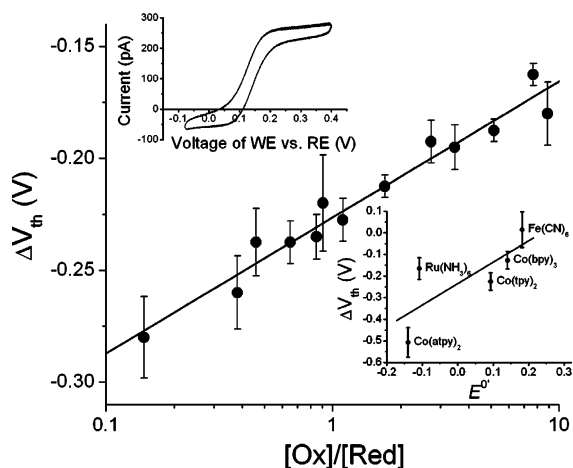


Figure 4. Threshold voltage shift for 100 μM $[\text{Co}(\text{tpy})_2]\text{Cl}_2$ with different $[\text{Ox}]/[\text{Red}]$ ratios, which are set by bulk electrolysis. The supporting electrolyte was 1 mM NaCl. Error bars show the standard deviation from four different NTs. The slope of the linear fit is 61 ± 6 mV. The $[\text{Ox}]/[\text{Red}]$ ratio was determined from the limiting currents measured from a cyclic voltammogram at a sweep rate of 25 mV/s, using a 25 μm Pt working electrode, a large-area Pt counter electrode, and a Ag/AgCl reference electrode, as shown in the upper inset. Oxidative and reductive diffusion-limited currents in this example were 270 pA and 56 pA, respectively, giving an $[\text{Ox}]/[\text{Red}]$ ratio of 0.21. The bottom inset shows that the threshold voltage shift varies roughly linearly with $E^{0'}$, the formal potential of the redox-active molecules, which was measured by cyclic voltammetry with a Ag/AgCl reference. The slope of the fit is 0.99 ± 0.49 .

is several times greater for the $[\text{Co}(\text{bpy})_3]^{2+/3+}$ and $[\text{Fe}(\text{CN})_6]^{3-/4-}$ redox couples.

The threshold voltage shift at $[\text{Ox}]/[\text{Red}] = 1$ was determined for all of the molecules. This is plotted in the lower inset of Figure 4 as a function of the formal potential $E^{0'}$ of each molecule, which is the potential at which

oxidation or reduction occurs versus the potential of a Ag/AgCl reference electrode. The data are consistent with a linear dependence of the threshold voltage shift on $E^{0'}$ with unit slope, but there is a large degree of scatter in the measurements so further tests need to be done to confirm this relationship.

To develop a quantitative model to understand these data, we first recall that the Nernst equation gives the chemical potential of the electrons in a solution of redox-active molecules with formal potential $E^{0'}$ as

$$\frac{\mu_i}{e} = E^{0'} + \frac{kT}{ne} \ln \frac{[\text{Ox}]}{[\text{Red}]} \quad (2)$$

where k is Boltzmann's constant, T is the temperature, n is the number of electrons transferred, and e is the electron charge.¹ We can substitute this expression into eq 1 to express the voltage, V_g , applied to the gold electrolyte-gate wire as

$$V_g = \frac{\bar{\mu}_i}{e} = \varphi + \left[E^{0'} + \frac{kT}{ne} \ln \frac{[\text{Ox}]}{[\text{Red}]} \right] \quad (3)$$

If the nanotube behaves as a reference electrode and senses only the electrostatic potential, φ , then the shift in the threshold voltage, ΔV_{th} , is the change in V_g needed to produce the same φ , which is just the change in μ_i/e . Because $n = 1$ for all our molecules, we can write the expected threshold voltage shift as

$$\Delta V_{\text{th}} = \Delta E^{0'} + (59.2 \text{ mV}) \log \frac{[\text{Ox}]}{[\text{Red}]} \quad (4)$$

The observed gate-voltage dependence of the SWNT FET conductance follows this expected variation with the chemical potential of the redox-active molecules. Figure 4 shows that for $[\text{Co}(\text{tpy})_2]\text{Cl}_2$ the threshold voltage varies as $\log [\text{Ox}]/[\text{Red}]$ with a slope within 3% of 59.2 mV. The lower inset in Figure 4 shows that the threshold voltage for all the molecules varies roughly linearly with $E^{0'}$ with a slope of approximately unity, although there is a large degree of scatter in these data. We reiterate that in this model the local interaction is between the redox-active molecules and the gate wire, and the proximity of the molecules to the NT is irrelevant, as confirmed by Figure 3.

The molecules that show a higher slope for ΔV_{th} versus $\log [\text{Ox}]/[\text{Red}]$ also show an anomalously large slope when we measure the open circuit potential versus $\log [\text{Ox}]/[\text{Red}]$. The open circuit potential is measured with a high impedance voltmeter between a working and reference electrode. Because this is another measure of the chemical potential, it should follow the same form as ΔV_{th} . It is not clear why these molecules showed an anomalously large slope (it may result from a mixed potential due to other complexes or from dissolved oxygen in the solution), but it appears that the nanotube device still simply detects the change in chemical potential in the solution.

Because the SWNT FET, like a reference electrode, measures only the electrostatic potential, φ , it should show

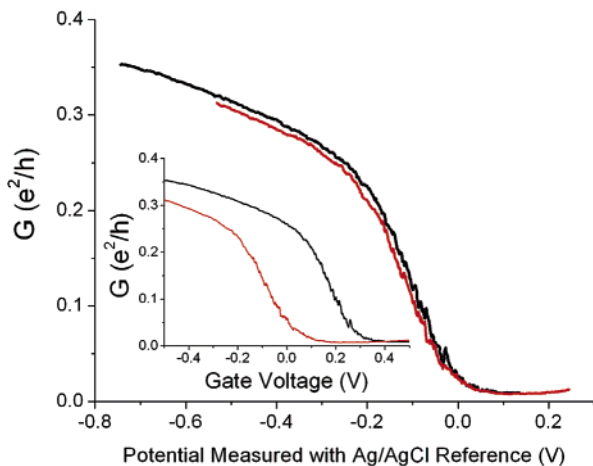


Figure 5. Nanotube conductance is almost identical in 1 mM NaCl (black) and in 100 μM of $[\text{Co}(\text{tpy})_2]\text{Cl}_2$ with a 1 mM NaCl supporting electrolyte (red) when plotted versus the potential measured with a Ag/AgCl reference electrode. The reference was inserted in the reservoir containing the gold gate wire. Inset: when the conductance is plotted versus the voltage applied to the gate wire, it shows a threshold voltage shift after the $[\text{Co}(\text{tpy})_2]\text{Cl}_2$ addition.

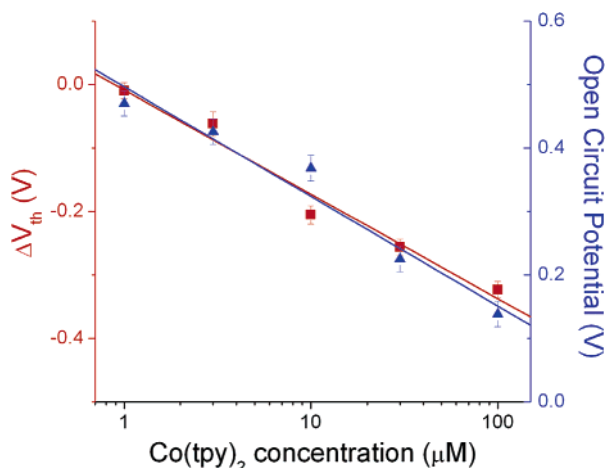


Figure 6. Threshold voltage shifts of SWNT FET (red squares, left axis) and open circuit potential between working and reference electrode (blue triangles, right axis) for $[\text{Co}(\text{tpy})_2]\text{Cl}_2$ at different concentrations, all in a 1 mM NaCl supporting electrolyte. Slope of fit is -164 ± 16 mV for threshold voltage data and -173 ± 21 mV for open circuit potential data.

no change relative to the potential measured with a reference electrode. To fully confirm this model, we measured the nanotube conductance versus the potential of a Ag/AgCl reference electrode before and after adding $[\text{Co}(\text{tpy})_2]\text{Cl}_2$ to the system, as shown in Figure 5. The molecules shifted the conductance as a function of the electrolyte-gate voltage, but there is virtually no conductance change as a function of the reference potential.

We now discuss the concentration dependence of the threshold voltage shift, which is shown in Figure 6 for $[\text{Co}(\text{tpy})_2]\text{Cl}_2$. The magnitude of the threshold voltage shift increases with the concentration, which has previously been interpreted as a sign of a local molecule-NT interaction.⁷ The open circuit potential, however, also varies with concentration, and both increases are logarithmic and have

roughly the same slope. Because both ΔV_{th} and the open circuit potential measure μ_i , we conclude that their concentration dependence simply reflects a changing μ_i and not molecule-NT adsorption. We have confirmed the variation of $[\text{Ox}]/[\text{Red}]$ with concentration by separate ultramicroelectrode measurements.

Figure 6 also shows that the minimum detectable concentration is about 1 μM , below which we see no shift. This may be caused by a second potential-determining couple present in the supporting electrolyte that dominates the mixed-potential at low concentrations. Adsorption of molecules to the electrolyte-gate wire or residual oxygen in the solution could also be affecting the measurements.

In conclusion, we have demonstrated that SWNT FETs can be used as nanoscale reference electrodes to measure the electrostatic potential of a solution. They can therefore detect changes in the chemical potential of solution due to redox-active transition-metal complexes, or in principle due to any potential-determining couple. These changes in potential shift the gate-voltage dependence of the nanotube conductance, and this shift depends linearly on the formal potentials of the molecules and logarithmically on their $[\text{Ox}]/[\text{Red}]$ ratios. Although there may also be some local interaction between the molecules and the nanotube, the primary source of the observed signal is this nonlocal electrochemical effect, which must be considered in any electrolyte-gated nanotube sensing experiment. The use of a SWNT FET as a reference electrode could lead to new kinds of nanoscale electrochemistry experiments and highly sensitive analytical strategies. For example, given that we can detect threshold voltage shifts down to 5 mV and concentrations down to 1 μM , we estimate that with a microfabricated electrolyte-gate electrode, we could detect a single redox event in a $[300 \text{ nm}]^3$ volume of solution.

Acknowledgment. This work was supported by the National Science Foundation through the NIRT program (Grant No. 0403806) and by the Nanobiotechnology Center (NBTC), an STC Program of the NSF under Agreement No. ECS-9876771. Sample fabrication was performed at the Cornell NanoScale Science and Technology Facility (a member of the National Nanotechnology Infrastructure Network), funded by the NSF.

Supporting Information Available: Chemical synthesis and purification of redox couples and experimental details for electrochemical measurements. This material is available free of charge via the Internet at <http://pubs.acs.org>.

References

- (1) Bard, A. J.; Faulkner, L. R. *Electrochemical Methods, Fundamentals and Applications*, 2nd ed.; John Wiley & Sons: New York, 2001.
- (2) Campbell, J. K.; Sun, L.; Crooks, R. M. *J. Am. Chem. Soc.* **1999**, *121*, 3779.
- (3) Heller, I.; Kong, J.; Heering, H. A.; Williams, K. A.; Lemay, S. G.; Dekker, C. *Nano Lett.* **2005**, *5*, 137.
- (4) Krüger, M.; Buitelaar, M. R.; Nussbaumer, T.; Schönenberger, C.; Forró, L. *Appl. Phys. Lett.* **2001**, *78*, 1291.

- (5) Rosenblatt, S.; Yaish, Y.; Park, J.; Gore, J.; Sazonova, V.; McEuen, P. L. *Nano Lett.* **2002**, *2*, 869.
- (6) Kong, J.; Franklin, N. R.; Zhou, C.; Chapline, M. G.; Peng, S.; Cho, K.; Dai, H. *Science* **2000**, *287*, 622.
- (7) Bradley, K.; Gabriel, J.-C. P.; Briman, M.; Star, A.; Grüner, G. *Phys. Rev. Lett.* **2003**, *91*, 218301.
- (8) Krüger, M.; Widmer, I.; Nussbaumer, T.; Buitelaar, M.; Schönenberger, C. *New J. Phys.* **2003**, *5*, 138.
- (9) Boussaad, S.; Tao, N. J.; Zhang, R.; Hopson, T.; Nagahara, L. A. *Chem. Commun.* **2003**, *13*, 1502.
- (10) Chen, R. J.; Choi, H. C.; Bangsaruntip, S.; Yenilmez, E.; Tang, X.; Wang, Q.; Chang, Y.-L.; Dai, H. *J. Am. Chem. Soc.* **2004**, *126*, 1563.
- (11) Bradley, K.; Briman, M.; Star, A.; Grüner, G. *Nano Lett.* **2004**, *4*, 253.
- (12) Fu, Q.; Liu, J. *Langmuir* **2005**, *21*, 1162.
- (13) Huang, S.; Woodson, M.; Smalley, R.; Liu, J. *Nano Lett.* **2004**, *4*, 1025.

NL060156I